Petrography and mineralogy of fault material from the Great Glen Fault

M. de Jongh, J. Rushton, R. Haslam, S.F. Parry, & S.J. Kemp
British Geological Survey (BGS), Keyworth, Nottingham, UK.

ABSTRACT: The Great Glen Fault (GGF) of Northern Scotland is a long-studied yet enigmatic fault structure. BGS interest in the movement history of the GGF, as part of a new UK-wide strategic initiative, has been stimulated by the Coire Glas project – a hydro-pumped storage scheme with the capability to double the current electricity storage capacity of Great Britain. This major civil engineering project will involve tunnelling through tectonised rocks associated with the GGF. Here, we outline a workflow for the characterisation of fault rocks using a fault gouge sample taken from the GGF close to the Coire Glas site. Our preliminary results show that the microstructure of the studied sample reflects a complex history of fracturing and related mineralization associated with movement on the GGF. We note that computerized tomography (CT) has proved a useful tool in confirming minimal disruption of the fault gouge material during sample preparation.

1 INTRODUCTION

The Great Glen Fault (GGF) is a major, long-lived, strike-slip fault with a NNE–SSW trend that extends across the mainland of Scotland, separating the Northern Highlands terrane to the north from the Grampian terrane to the south (Figure 1) (Strachan et al. 2002). The history of the structure is understood to include sinistral movement in the Devonian, dextral movement in the Carboniferous, with further reactivation during the Permian and Mesozoic. The fault remains seismically active (Allen 2019), and is thus an important geological structure to understand, especially with regards to civil engineering projects in the area. Despite repeated study over the last 180 years, the faulting history of the GGF is still debated (Miller 1841; Murchison & Geikie 1861; Horne & Hinxman 1914; Richey 1939; Kennedy 1946; Shand 1951; Marston 1967; Munro 1973; Pankhurst 1979; Underhill & Brodie 1993; Stewart et al 2001; Le Breton 2013; Searle 2022; Becker 2023). For a comprehensive review of the existing literature see Allen (2019).

‘UK structure’ is a new British Geological Survey (BGS) initiative that aims to characterise faults and fault rock across the UK, generating a baseline dataset that will meet the needs of stakeholders requiring information about the properties and movement history of faults in the UK and their impact on national infrastructure, groundwater resources and geodisposal. The Coire Glas Project, an ambitious renewable energy project which will be the first large-scale pumped hydro storage scheme in the UK in over 40 years and has the potential to double the electricity storage capacity in the UK (SSE 2023), serves as an excellent example of a scheme demanding such information. The project site is broadly located on the northern shore of Loch Lochy, with the proposed upper reservoir to be built within Coire Glas itself (Figure 1) and the proposed outflow into Loch Lochy lying approximately 3 km SW of Kilfinnan Farm. Delivery of the scheme will involve tunnelling through part of the GGF in order to connect the lower reservoir (Loch

Lochy) with the new upper reservoir. The site of the proposed upper reservoir within Coire Glas is underlain by the heterolithic Tarvie Psammite Formation (Loch Ness Supergroup). This consists of variable proportions of psammite, minor semipelite, and rare amphibolite. There are a number of minor intrusions within the Tarvie Psammite Formation, including granitic dykes inferably associated with the Caledonian Orogeny and mafic dykes of Carboniferous age. The GGF in this area is mapped as a broad zone of cataclastic rock, striking NNE–SSW, with a width of up to 4 km. The fault comprises a series of highly deformed shear zones of mylonite, cataclasite, and fault gouge surrounding entrained blocks of wall rock of various compositions, which themselves show lesser degrees of deformation (protobreccia to protocataclasite).

The objective of this paper is to demonstrate an analytical workflow developed at BGS aimed at determining the petrography and mineralogy of fault rocks. Here, as an example, we present the preliminary findings of the analysis of a polished thin section prepared from fault gouge material collected from the GGF in the Coire Glas area. As well as describing the mineralogy and petrography, we comment on the value of CT scanning as a means of confirming minimal disruption during oriented sample preparation. The workflow will be applied to further samples from the GGF, and other UK faults, as part of BGS' structural research programme.

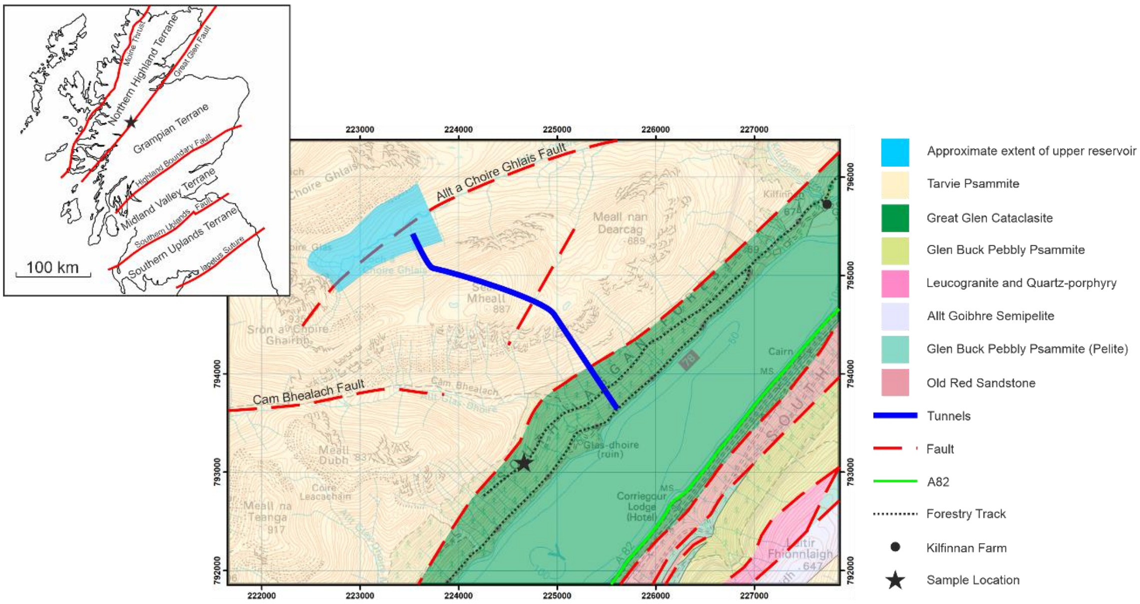

Figure 1. Major faults and terranes in Scotland (after Strachan et al. 2002). The Coire Glas project site is located between Fort William and Fort Augustus, on the NE–SW oriented Great Glen Fault. The project infrastructure will be constructed within rocks of the Tarvie Psammite Formation (Loch Ness Supergroup) and a broad zone of 'Great Glen Cataclasite' (Geology simplified from BGS Geology 50K (DigMapGB-50) © UKRI. Contains Ordnance Survey data © Crown Copyright and database rights 2023. Ordnance Survey Licence OS AC0000824781)

2 SAMPLING

The sample reported on here was collected from a drainage ditch along the upper forestry track that runs parallel to Loch Lochy (British National Grid [224653,793078]). The site is located in the NE part of an area mapped as 'Great Glen Catalasite'. The sample was collected using 50 mm square aluminium 'box' with a length of 100 mm and a wall thickness of 2 mm. Aluminium was chosen for sampling purposes to minimize the chance of metal leaching into the sample and for its low density, which permits better imaging within a CT Scanner. The sample box was hammered into the *in situ* clay gouge and the box then excavated using a trowel to minimise damage to the sample material. The orientation of the sample was inscribed on the aluminum box before removal, and the sample was wrapped in plastic film and sealed with packing tape to retain moisture content.

The sample itself consists of a blue-grey fault gouge (which weathers to orange at surface) between bands of psammitic wall rock, and parallel to the strike of the GGF. The gouge has several minor internal shear planes corresponding to Riedel shears and contains an entrained, lensoidal, block of psammitic wall rock, which are generally consistent with a dextral sense of the fault movement.

3 METHODS

3.1 *Sample preparation (thin sectioning and CT scanning)*

We used a GeoTech RXCT (Rotating X-ray Computed Tomography) to capture the condition and orientation of the fault gouge material prior to preparation of a polished thin section. Approximately 1400 scan slices were analysed using the following CT scanning operating conditions: copper filter; voltage 135 kV and current 100 mA; 85 µm/pixel resolution.

The aluminium box containing the fault gouge sample was cut using a hand saw to avoid disturbing the material through excessive vibration. After cutting, CT was used to characterise the sample material within the aluminium box. Two polished thin sections (PTS) of the cut sample, henceforth referred to as H1 and H2, were then prepared using standard thin sectioning procedures at the BGS. The section was prepared to 100 µm thickness to facilitate future laser work. Finally, images of the PTS were compared to the CT scan data to allow for comparison and identification of potential disturbance during sample preparation.

3.2 *Scanning Electron Microscopy (SEM)*

SEM was used to characterise sample H2, including textural properties and cross-cutting relationships. A Mineralogic© phase map was also created, thereby revealing the relationship between different mineral phases. SEM analysis was carried out using a Zeiss Sigma 300 field emission gun scanning electron microscope (FEG-SEM) fitted with twin Bruker X-flash energy-dispersive X-ray (EDX) detectors and running Zeiss' Mineralogic© phase mapping software (version 1.6.2). Samples were examined under high vacuum conditions (10–4 Pa), at an accelerating voltage of 20 keV with a 120 µm aperture. BSE images were captured with accompanying EDX-derived element maps using Bruker Esprit (v2.1) software.

3.3 *Optical (cold-cathode) cathodoluminescence (CC-CL)*

CC-CL applied to fault rocks reveals textures that are usually not visible using methods such as optical microscopy and scanning electron microscopy (SEM). The optical CL system provides 'true' colour CL and uses a defocused stationary beam making it an ideal set up for analysis of minerals displaying phosphorescence. In this study, we used a NewTech Cathodyne CC-CL system operating at 12 kV and 50 µA.

3.4 *X-ray Diffraction (XRD)*

Mineralogy of the fault gouge sample was characterized using a PANalytical X'Pert Pro diffractometer (Malvern Panalytical Ltd., Malvern, UK) equipped with Co-Kα radiation ($\lambda = 1.78896$ Å) and operated at 45 kV and 40 mA. Crystalline minerals were identified using PANalytical HighScore Plus software (v. 5.1) coupled to the International Centre for Diffraction Data PDF-4+ database (International Centre for Diffraction Data (ICDD), 2023). Quantification of relative mineral proportions was completed using the Rietveld refinement technique within the same HighScore Plus software package using crystallographic information from the Inorganic Crystal Structure Database (Hellenbrandt, 2004; Inorganic Crystal Structure Database (ICSD), 2023) (see Kemp et al 2016a for more detail).

The clay fraction (< 2µm) was separated and analysed in order to better understand the clay mineralogy. More detail on the procedure used to separate and analyse the clay fraction can be found in Kemp et al (2016b).

4 RESULTS AND DISCUSSION

CT provided a means of capturing the orientation of grains within the sample prior to preparation of a PTS. The CT scans were visually compared with the PTS to determine if any disturbance had occurred during sample preparation. Sample H1 showed rotation of various grains along multiple axes (Figure 2b) and had thus been ‘deformed’ during sample preparation. However, H2 appeared almost identical to the CT scan suggesting minimal to no ‘deformation’ during sample preparation. Use of CT has clearly demonstrated that fault gouge samples are susceptible to ‘deformation’ during sample preparation.

The mineralogy of the fault gouge sample determined by XRD is summarised in Table 1. The whole rock mineralogy is primarily composed of undifferentiated mica species, quartz, and dolomite. Relatively minor components include kaolin-group minerals, anatase (Ti oxide), siderite, and pyrite, and the <2 µm clay-sized fraction was composed mostly of *R*1 ordered illite/smectite.

The Mineralogic© output (Figure 3a) shows fractured psammite clasts with dolomite veins, supported within a gouge matrix composed primarily of clay minerals, muscovite, and other silicates. Five distinguishable types of fracture-associated mineralisation were identified: Fe-dolomite cement associated with the clasts (multiple cross-cutting episodes); Mg-rich siderite cement within fault gouge matrix; fine kaolin within fractures of clasts; coarse kaolin within fractures of clasts; and calcite cement within fractures of clasts (Figure 3a-e). Two types of kaolin cements were identified based on their morphological properties. The first type appears very fine-grained and tightly packed, while the second type appears coarsely crystalline (Figure 3c).

The relative timings of mineralisation types have been interpreted as follows. The first phase of *in-situ* growth is associated with the formation of Fe-dolomite within clasts (Figure 3a,d) and Mg-siderite found primarily within the gouge matrix (Figure 3a,b). Mg-siderite occurs within and around smaller fragments of wall rock indicating that it post-dates incorporation of wall rock fragments in the fault gouge (Figure 3e). Dolomite fragments and Mg-siderite appear to have been subsequently deformed together within a ductile regime as evidenced by a boudinage texture (Figure 3e). This is then followed by a relatively later episode of brittle fracturing shown by brittle fracturing of Mg-siderite bands within gouge matrix and fracturing of wall rock fragments (fracturing which clearly crosscuts earlier Fe-dolomite filled fractures) (Figure 3d). This episode of brittle fracturing is also evidenced by CL observations, which show offset in growth zones of dolomite (Figure 3f,g). This episode was followed by Fe-dolomite mineralization as fracture wall overgrowths, which has been subsequently cemented by kaolin and calcite. In places, there is evidence for calcite partially replacing (and therefore post-dating) the kaolin cement (Figure 3c).

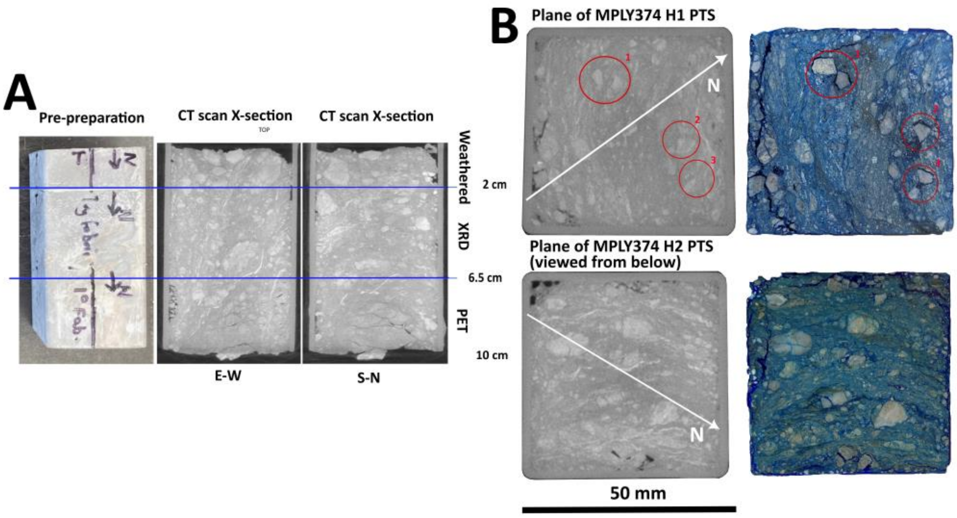

Figure 2. A= CT scans of entire sample (MPLY374); B = slices which were prepared as thin sections, H1 and H2. Comparison between CT scan prior to preparation of PTS, and image of PTS after preparation. Deformation during sample preparation of sample H1 highlighted with red circles.

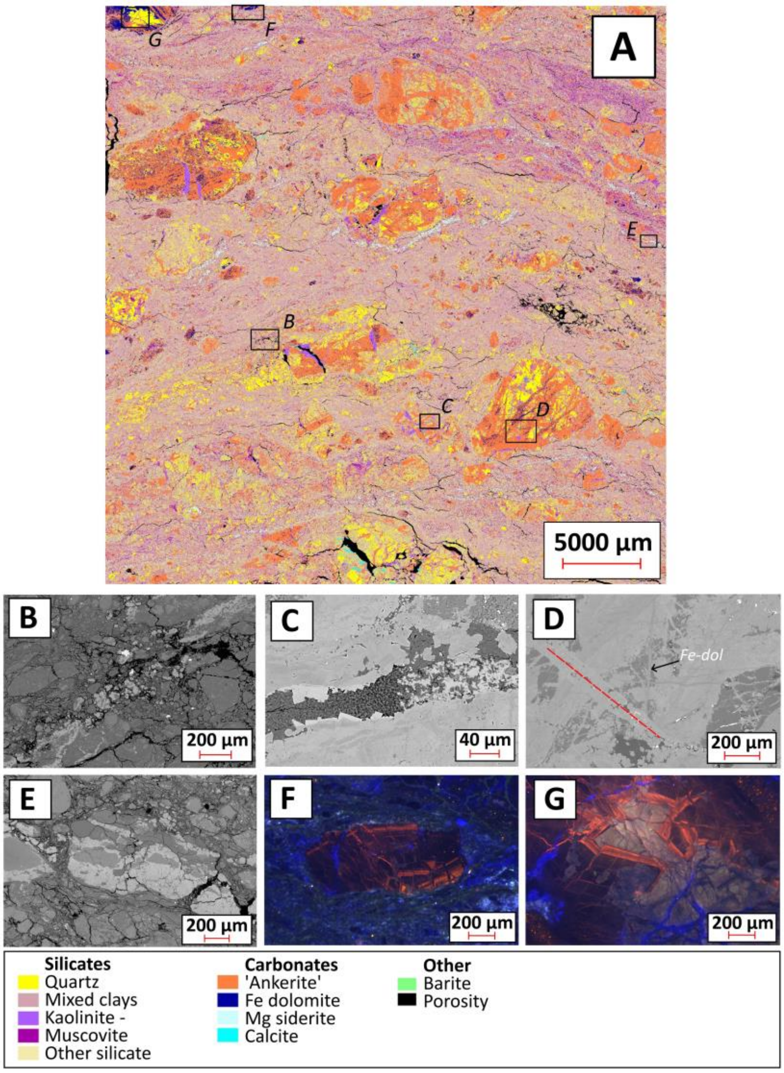

Figure 3. Petrography of fault gouge sample. A = Mineralogic© map showing distribution of mineralogy within sample (key at base of figure, the term 'ankerite' is used informally to differentiate dolomite with the highest Fe contents). B = BSE image showing brittle fracturing of siderite cement; C = BSE image showing different phases of kaolin, dolomite and calcite cements; D = high contrast BSE image showing cross cutting relationships observed in wall rock fragment. Note fracture highlighted which postdates all other fracturing in clast and also extends into the gouge suggesting it occurred relatively later; E = BSE image showing fractured dolomite cemented by siderite, which has in turn been deformed into a boudinage texture; F = CL image of wall rock fragment showing offset in growth zones (dolomite is orange-red); G = high magnification CL image of wall rock fragment showing minor offset observed in growth zones associated with Fe-dolomite followed by mineralisation of kaolin in fractures.

	Whole rock powder (%)	< 2 µm oriented (%)
Mica species*	38.4	
Quartz	27.4	
Dolomite	23.0	
Kaolin	4.6	10.0
Anatase	3.0	
Siderite	2.8	
Pyrite	0.8	
Illite/smectite		82.0
Illite		8.0

*Undifferentiated

Table 1. XRD mineralogy results for whole rock powder and clay fraction (< 2 µm oriented).

5 CONCLUSIONS

Preliminary analysis of a fault gouge sample from the GGF using a workflow developed at the BGS aimed at better-characterising fault rocks has not only established the compositional make-up and mineralisation history of the fault rock, but has demonstrated the value of CT in ensuring preparation of an undisturbed sample. Overall, the studied GGF fault gouge shows a complex history, with several phases of mineralisation that are associated with at least two separate fracturing events. Dating of the constituent calcite and clay minerals will potentially provide key temporal constraints on the overall faulting history of the GGF.

6 REFERENCES

Allen, M. 2019. The long and moving story of the Great Glen Fault. *Mercian Geologist*, *19*(4), 216.

Becker, C. 2023. Shearing on the Great Glen Fault: Kinematic and Microstructural Evidence Preserved at Different Crustal Levels (*Doctoral dissertation, Virginia Tech*).

Horne J., & Hinxman L.W. 1914. The geology of the country round Beauly and Inverness. Mem. *Geol. Surv. GB.*

Kemp, S.J., Smith, F.W., Wagner, D., Mounteney, I., Bell, C.P., Milne, C.J., Gowing, C.J. B., Pottas, T.L., 2016. An improved approach to characterize potash-bearing evaporite deposits, evidenced in North Yorkshire, United Kingdom. *Econ. Geol.* 111, 719–742. https://doi.org/10.2113/econgeo.111.3.719.

Kemp, Simon J., Ellis, M.A., Mounteney, I., Kender, S. 2016. Palaeoclimatic implications of high-resolution clay mineral assemblages preceding and across the onset of the Palaeocene–Eocene Thermal Maximum, North Sea basin. *Clay Miner*. 51, 793–813. https://doi.org/10.1180/claymin.2016.051.5.08.

Kemp, S.J., Gillespie, M.R., Leslie, G.A., Zwingmann, H. And Campbell, S.D.G. 2019. Clay mineral dating of displacement on the Sronlairig Fault: implications for Mesozoic and Cenozoic tectonic evolution in northern Scotland. *Clay Minerals,* 54, 181–196.

Kennedy, W. Q. 1946. The great glen fault. *Quarterly Journal of the Geological Society*, *102*(1-4), 41-76.

Le Breton E., Cobbold P.R., & Zanella A., 2013. Cenozoic reactivation of the Great Glen fault, Scotland: additional evidence and possible causes. *J. Geol. Soc.*, 170, 403-415

Linzmeier, B., Kitajima, K., Denny, A., & Cammack, J. 2018. Making maps on a micrometer scale, *Eos*, 99, https://doi.org/10.1029/2018EO099269.

Marston R.J. 1967. Newer granites of Foyers and Strontian and the Great Glen fault. *Nature*, 214, 159-161

Miller H. 1841. The Old Red Sandstone. *Johnstone: Edinburgh*

Munro M. 1973. Structures in the south-eastern portion of the Strontian granitic complex, Argyllshire. *Scot. J. Geol*., 9, 99-108.

Murchison R.I., & Geikie A. 1861. On the altered rocks of the Western Islands of Scotland, and the North-Western and Central Highlands. *Q. J. Geol. Soc.*, 17, 171-240.

Pankhurst R.T. 1979. Isotope and trace element evidence for the origin and evolution of Caledonian granites in the Scottish Highlands. 18-33 in *Atherton H.P. & Tarney J*. (eds.), Origin of granitic batholiths, *Springer: Berlin*.

Richey J.E. 1939. The dykes of Scotland. Trans. *Edinburgh Geol. Soc*., 13, 395-435.

Searle, M. P. 2022. Reply to Dewey and Ryan Comment on Searle, MP (2021)'Tectonic evolution of the Caledonian orogeny in Scotland: a review based on the timing of magmatism, metamorphism and deformation'. *Geological Magazine*, *159*(10), 1837-1845.

Shand S.J. 1951. Mylonite, slickensides and the Great Glen fault. *Geol. Mag*., 88, 423-428

SSE Renewables. 2023. Coire Glas: Helping Scotland and the UK deliver net zero. 1-10

Stewart M., Strachan R.A., Martin M.W. & Holdsworth R.E. 2001. Constraints on early sinistral displacements along the Great Glen fault zone, Scotland: structural setting, U-Pb geochronology and emplacement of the syn-tectonic Clunes tonalite. *J. Geol. Soc*., 158, 821-830.

Strachan, R.A, Harris. A.L, Fettes, D.J and Smith, M. 2002. The Highland and Grampian terranes. In The Geology of Scotland, 4th edition (ed. NH Trewin), pp. 81–148. *London: The Geological Society*.

Underhill, J. R., & Brodie, J. A. 1993. Structural geology of Easter Ross, Scotland: implications for movement on the Great Glen fault zone. *Journal of the Geological Society*, *150*(3), 515-527.